Digital 2D wavefield reconstruction based on novel two-matrix forward/backward propagation modeling

Vladimir Katkovnik, Artem Migukin, Jaakko Astola, and Karen Egiazarian

Department of Signal Processing, Tampere University of Technology (TUT)
Korkeakoulunkatu 10, P. O. Box 553, Tampere, FI-33720 Tampere
Tel. +358 (0)3 3115 11, Fax +358 3 3115 4989, E-mail: firstname.lastname@tut.fi

Abstract

An application area of digital holography continuously extends: three-dimensional imaging, laser projections, material processing, deformation detection, microscopy, etc. A wavefield reconstruction from intensity and/or phase measurements is one of the basic problems in digital holography methods [1]. We consider reconstruction of a wavefield distribution in an object plane from data in a diffraction (sensor) plane. In this paper we discuss and study a novel two-matrix digital model for the forward wavefield propagation originated in [2]. This model is aliasing free and precise for pixel-wise invariant object and sensor plane distributions. Following [2-3] we use this model for formalization of the object wavefield reconstruction (backward propagation) as an inverse problem. Depending on the parameters of the optical setup this problem can be very ill-conditioned. Main results of this paper concern the study of the conditioning of the problem and its link with the accuracy of the wavefield reconstruction. We select a regularizing parameter using the condition number of the transfer matrices of the proposed model. Simulation experiments demonstrate a very good performance of the developed wavefield reconstruction technique in comparison with the conventional convolutional and discrete Fresnel transform algorithms.

Keywords: wavefield reconstruction, Fresnel approximation, inverse problems

1. Introduction

In a typical holography setup there are two different planes: input (object) and output (sensor) ones (Fig. 1). The object plane is a source of light radiation or reflection (according to the type of an object: diffusely passing or reflecting one) propagating along the optical axis and the output plane (with an imaging CMOS sensor) which is parallel to the object plane with a distance *d* between the planes.

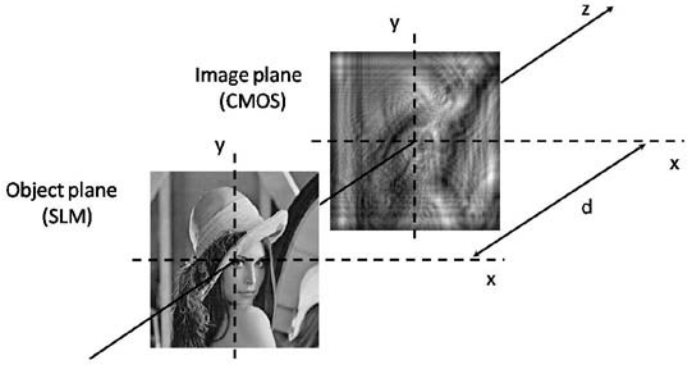

Fig.1. Principal setup of wavefield propagation and reconstruction

This paper concerns a digital modeling for both forward and backward wavefield propagations. For the forward propagation we use a novel algebraic approach based on the matrix transform of the wavefield distributions proposed in [2]. It is assumed that an object distribution is pixel-wise invariant, and then there is an accurate discrete-to-discrete model

linking discrete values of the wavefield distributions averaged over pixels in the object and sensor planes. This modeling is aliasing free and accurate for pixel-wise invariant object and sensor distributions. The reconstruction of the object distribution from a distribution given in the sensor plane is formulated as an inverse problem [2]. Depending on the pixel size and the distance between the object and sensor planes the matrices of the introduced Matrix Discrete Diffraction Transform (M-DDT) can become very ill-conditioned what makes the reconstruction of the object distribution difficult or even impossible. The possibility of a perfect/good quality reconstruction is well characterized by the rank and conditioning number of the transform matrices. The forward matrix transform modeling is a natural and very productive tool to study limitations of the wavefield reconstruction and to develop novel effective algorithms. In this paper we introduce a regularized inverse reconstruction algorithm based on the M-DDT, study the conditioning of the inverse problem depending on the parameters of the optical setup and connect this conditioning number with the accuracy of the wavefield reconstruction.

2. Modeling of wavefield propagation

Let us define a 2D complex-valued wavefield $u_o(x,y)$ in the object plane *(x,y,0)* as a function of the lateral coordinates *x* and *y*. According to the scalar diffraction theory [4] there is a linear operator which allows calculating a wavefield distribution $u_z(x,y)$ in the sensor plane as $u_d(x,y)=\mathcal{D}_d\{u_o\}$, where $\mathcal{D}_d$ stands for a diffraction operator $\mathcal{D}_z$ with a distance parameter $z=d$:

$$u_z(x,y)=\mathcal{D}_z\{u_o\}=\int_{-\infty}^{\infty}\int_{-\infty}^{\infty} g_z(x-\xi,y-\eta)u_o(\xi,\eta)d\xi d\eta\,,\ z>0\,, \tag{1}$$

where $(x,y)\in R^2$, the kernel $g_z(x,y)$ is shift invariant and has a form of the first Raylegh-Sommerfeld solution of the Maxwell-Helmholtz equation. Here $k=2\pi/\lambda$ is a wavenumber and λ is a wavelength. If the distance *d* is much larger than the wavelength than the kernel in (1) is of the form:

$$g_z=z\cdot\frac{\exp(j2\pi\cdot r/\lambda)}{j\lambda r^2},\ r=\sqrt{x^2+y^2+z^2},\ z>>\lambda\,. \tag{2}$$

If $z>>x,y$ the Fresnel approximation of this kernel can be represented as

$$g_z=\frac{\exp(j2\pi\cdot z/\lambda)}{j\lambda z}\exp(j\frac{\pi}{\lambda z}[x^2+y^2])\,. \tag{3}$$

It is proved that the operator $\mathcal{D}_z$ is invertible, and this inverse operator also can be presented as a convolution with a shift-invariant kernel. If the diffraction wavefield $u_z(x,y)$ is given the wavefield in the object plane *z=0* can be reconstructed using the inverse operator $\mathcal{D}_z^{-1}$:

$$u_o(\xi,\eta)=\mathcal{D}_z^{-1}\{u_z\}=\int_{-\infty}^{\infty}\int_{-\infty}^{\infty} g_{-z}(\xi-x,\eta-y)u_z(x,y)dxdy\,. \tag{4}$$

In contrast to standard techniques, which consider discrete models as approximations for the forward and backward wavefield propagation integrals, we follow a different idea. We start from an accurate forward propagation discrete modeling which is precise for a class of pixel-wise invariant distributions and then reconstruct the object distribution by inverting this precise forward model. The main point is that for the wavefield reconstruction we do not use the backward propagation integral (4), which is valid for the infinite sensor only. A derivation and theory of the DDT in frequency and space domains can be found in [2-3].

3. M-DDT representation

Let images and pixels in the object and sensor planes are rectangular and have the following sizes: $N_{y,0} \times N_{x,0}, \Delta_{y,0} \times \Delta_{x,0}$ and $N_{y,z} \times N_{x,z}$, $\Delta_{y,z} \times \Delta_{x,z}$, respectively. Then, the space domain DDT can be introduced as follows [2]:

$$u_z[k,l] = \sum_{s=-N_{y,0}/2}^{N_{y,0}/2-1} \sum_{t=-N_{x,0}/2}^{N_{x,0}/2-1} a_z(k,s;l,t) u_o[s,t], \;\; k = -\frac{N_{y,z}}{2} \ldots \frac{N_{y,z}}{2} - 1, \;\; l = -\frac{N_{x,z}}{2} \ldots \frac{N_{x,z}}{2} - 1, \quad (5)$$

where the kernel a_z, in general, can be shift-varying:

$$a_z(k,s;l,t) = \frac{1}{\Delta_{y,z}\Delta_{x,z}} \int_{-\Delta_{y,z}/2}^{\Delta_{y,z}/2} \int_{-\Delta_{y,0}/2}^{\Delta_{y,0}/2} \int_{-\Delta_{x,z}/2}^{\Delta_{x,z}/2} \int_{-\Delta_{x,0}/2}^{\Delta_{x,0}/2} g_z(k\Delta_{y,z} - s\Delta_{y,0} + \xi + \xi', l\Delta_{x,z} - t\Delta_{x,0} + \eta + \eta') d\xi d\xi' d\eta d\eta' \quad (6)$$

For the Fresnel approximation of g_z the kernel a_z allows the following factorization:

$$a_z(k,s;l,t) \cong \mu \cdot \mathbf{A}_y(k,s) \cdot \mathbf{A}_x(l,t), \;\; \mu = \frac{\exp(j2\pi \cdot z/\lambda)}{j\lambda \cdot z}, \quad (7)$$

where the transfer matrices $\mathbf{A_y}$ and $\mathbf{A_x}$ are calculated according to the formulas:

$$\mathbf{A}_x(l,t) = \frac{1}{\Delta_{x,z}} \int_{-\Delta_{x,z}/2}^{\Delta_{x,z}/2} \int_{-\Delta_{x,0}/2}^{\Delta_{x,0}/2} \exp[\frac{j\pi}{\lambda z}(l\Delta_{x,z} - t\Delta_{x,0} + \eta + \eta')^2] d\eta d\eta', \quad (8)$$

$$\mathbf{A}_y(k,s) = \frac{1}{\Delta_{y,z}} \int_{-\Delta_{y,z}/2}^{\Delta_{y,z}/2} \int_{-\Delta_{y,0}/2}^{\Delta_{y,0}/2} \exp[\frac{j\pi}{\lambda z}(k\Delta_{y,z} - s\Delta_{y,0} + \xi + \xi')^2] d\xi d\xi'. \quad (9)$$

Inserting (7) into (5) we arrive to the "*Matrix Digital Diffraction Transform*" (M-DDT) model for the forward wavefield propagation presented in the form:

$$\mathbf{u}_z = \mu \cdot \mathbf{A}_y \cdot \mathbf{u}_o \cdot \mathbf{A}_x^T, \quad (10)$$

where $\mathbf{u}_o(x,y)$ and $\mathbf{u}_z(x,y)$ are the complex-valued matrices of wavefield distributions in the object and image planes.

4. Backward (inverse) modeling

In order to solve (10) with respect to $\mathbf{u}_o(x,y)$ the standard Tikhonov regularization technique is used. We are looking for a regularized estimate of $\mathbf{u}_o$ defined as a minimizer of the quadratic criterion:

$$\hat{\mathbf{u}}_o = \arg\min_{\mathbf{u}_o} \{ \| \mathbf{u}_z - \mu \cdot \mathbf{A}_y \cdot \mathbf{u}_o \cdot \mathbf{A}_x^T \|_F^2 + \alpha \| \mathbf{u}_o \|_F^2 \} \quad (11)$$

Here $\| \cdot \|_F^2$ is the quadratic Frobenius matrix norm, and $\alpha \geq 0$ controls the level of regularization or smoothness of $\hat{\mathbf{u}}_o$. Minimization of (11) gives the solution in the form:

$$\hat{\mathbf{u}}_o = \mu^* \mathbf{B}_y \mathbf{A}_y^H \mathbf{u}_z \mathbf{A}_x^* \mathbf{B}_x + \alpha |\mu| \mathbf{B}_y \hat{\mathbf{u}}_o \mathbf{A}_x^T \mathbf{A}_x^* \mathbf{B}_x + \alpha |\mu| \mathbf{B}_y \mathbf{A}_y^H \mathbf{A}_y \hat{\mathbf{u}}_o \mathbf{B}_x, \quad (12)$$

where $\mathbf{B}_y = (|\mu| \mathbf{A}_y^H \mathbf{A}_y + \alpha \mathbf{I})^{-1}$, $\mathbf{B}_x = (|\mu| \mathbf{A}_x^T \mathbf{A}_x^* + \alpha \mathbf{I})^{-1}$ and $(\cdot^{\mathrm{H}})$ stands for the Hermitian conjugate. It has been checked numerically that the second and the third components in the right-hand side of this equation are not essential and can be dropped. In this case the approximate regularized inverse solution can be represented as

$$\hat{\mathbf{u}}_o = \mu^* (|\mu| \mathbf{A}_y^H \mathbf{A}_y + \alpha \mathbf{I})^{-1} \mathbf{A}_y^H \mathbf{u}_z \mathbf{A}_x^* (|\mu| \mathbf{A}_x^T \mathbf{A}_x^* + \alpha \mathbf{I})^{-1} \quad (13)$$

5. Numerical experiments and their analysis

It is assumed that images in object and sensor planes are squared and can be of a different size: $N_{y,0} = N_{x,0} = N_0$ and $N_{y,z} = N_{x,z} = N_z = qN_0$, where the parameter $q \geq 1$ shows a ratio of the image sizes in the sensor and object planes. The following values of the parameters are

assumed in our experiments: $\lambda = 632.8\,\text{nm}$, $\Delta_z = \Delta_0 = 7.4\,\mu\text{m}$, $N_0 = 512$ pixels. The root mean square error (*RMSE*) is used as an accuracy criterion. Following [2], we introduce "*in-focus*" distance defined by the formula $d_f|_q = N_z \cdot \Delta_z \cdot \Delta_0 / \lambda = q \cdot N_0 \cdot \Delta_z \cdot \Delta_0 / \lambda$, as a distance when the perfect reconstruction of $\hat{\mathbf{u}}_o$ is possible for the sensor size $N_z = qN_0$. This distance is originated from the Fresnel diffraction transform defining the conditions when FFT is applicable for calculations.

The "Lena" test-image is used in our experiments for amplitude modulation of the object wavefield distribution. It is assumed that the wavefield in the object plane is complex-valued with an invariant phase and amplitude equal to the intensity of the "Lena" test-image. The complex-valued observations in the sensor plane are used for reconstruction of this amplitude distribution. We compare the following algorithms: the M-DDT defined by the formula (13), the frequency domain DDT (F-DDT) [3], the convolutional inverse using the transfer function with original (conv1) and double (conv2) image sizes as it is defined in [2], and the inverse discrete Fresnel transform (IDFrT).

Depending on parameters the matrices $\mathbf{A}_y^H \mathbf{A}_y$ and $\mathbf{A}_x^* \mathbf{A}_x^T$ can be extremely ill-conditioned, then the regularization parameter α in the matrices $\mathbf{B}_x$ and $\mathbf{B}_y$ is of importance. We select the regularization parameter recursively starting from very small values α up to the moment when the conditioning number becomes smaller then the critical value equal to 10^6.

Fig.2. Original image (a) and image reconstructions by: (b) M-DDT, *RMSE*=0.027, (c) F-DDT , *RMSE*=0.029, (d) IDFrT, *RMSE*=0.064.

Visual and numerical comparisons of the algorithms are presented in Fig. 2 for the equal sizes of the object and sensor images (q=1) and for the distance $z = 3 \cdot d_f|_{q=1}$. A numerical accuracy comparison of all considered algorithms as a function of the distance d (for q=1) is produced in Fig. 3. The advantage of the M-DDT over the conventional algorithms is obvious.

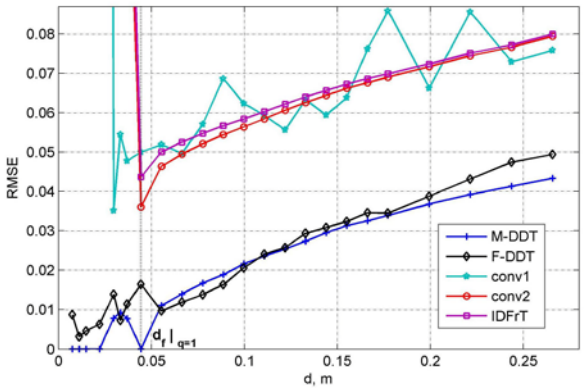

Fig.3. The accuracy of the image restoration (RMSE) versus the distance d for different algorithms

A larger sensor size (q>1) results in a better accuracy for the M-DDT reconstruction. In Fig. 4 we show how the accuracy of this reconstruction depends on the parameter q (Fig. 4b) and link this accuracy with the conditioning (*cond*) of the matrices $\mathbf{A}_y^H\mathbf{A}_y$ or $\mathbf{A}_x^*\mathbf{A}_x^T$ (Fig. 4a). In our case, for the matrices $\mathbf{A}_y$ and $\mathbf{A}_x$, which have the same size, the condition numbers have the equal value. This value is small for all sensor sizes, q={1,2,4}, if the distance d is smaller or equal to the corresponding "*in-focus*" distance $d_f|_q$, i.e. $d \le d_f|_q$. For these "smaller" distances we obtain a high-accuracy (nearly perfect) reconstruction (see Fig. 4b). As soon as $d > d_f|_q$ the condition number grows rapidly and the accuracy of reconstruction is correspondingly going down. A similarity in behavior of the curves in Fig. 4a and Fig. 4b confirms that a study of the conditioning number gives a clear indication of the accuracy of reconstruction and can be used for optimization of optical setups and sensors.

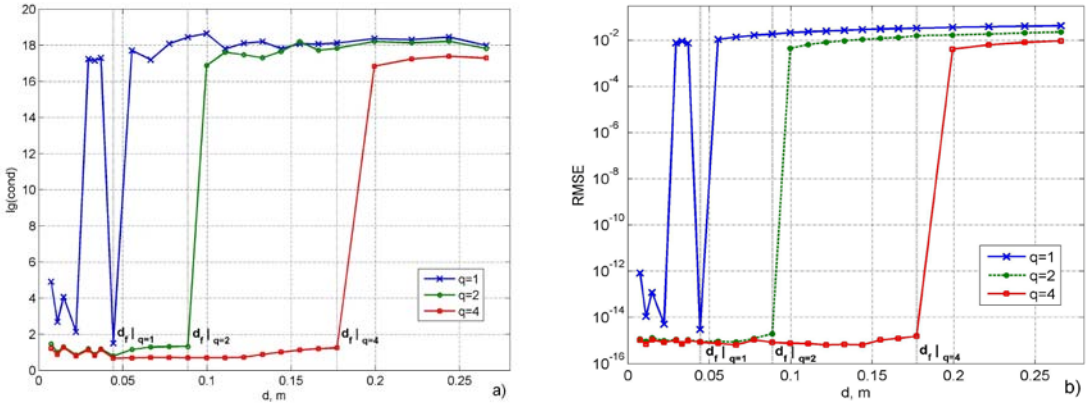

Fig.4. (a) Condition numbers *cond* (in log scale) and (b) *RMSE* versus the distance d for q={1, 2, 4}.

6. Conclusion

This paper concerns a novel two-matrix digital model for forward wavefield propagation. The condition number of the matrices can be used as indication of a potential accuracy which could be achieved for object wavefield reconstruction. Simulation experiments show the significant numerical and visual advantage of the M-DDT algorithm versus the standard convolutional and discrete Fresnel transform algorithms. The recursive F-DDT reconstruction demonstrates the accuracy close to given by the M-DDT algorithm.

7. Acknowledgments

This research was supported by the Academy of Finland, project No. 213462 (Finnish Centre of Excellence program 2006 - 2011).

References

1. Th. Kreis, *Handbook of Holographic Interferometry (Optical and Digital Methods)*, Wiley-VCH Gmbh&Co.KGaA, Weinheim, 2005.
2. Vladimir Katkovnik, Artem Migukin, Jaakko Astola, *"Backward discrete wavefield propagation modeling as an inverse problem: toward perfect reconstruction of wavefield distributions"* Appl. Opt, submitted 2008, http://www.cs.tut.fi/~lasip.
3. V. Katkovnik, J. Astola, and K. Egiazarian, *"Discrete diffraction transform for propagation, reconstruction, and design of wavefield distributions,"* Appl. Opt. **47**, 3481-3493 (2008).
4. J. W. Goodman, *Introduction to Fourier Optics.* McGraw-Hill Inc, New York, Second Edition, 1996.